

# SCIENTIFIC REPORTS



OPEN

## DkXTH8, a novel xyloglucan endotransglucosylase/hydrolase in persimmon, alters cell wall structure and promotes leaf senescence and fruit postharvest softening

Received: 07 June 2016  
Accepted: 18 November 2016  
Published: 14 December 2016

Ye Han\*, Qiuyan Ban\*, Hua Li, Yali Hou, Mijing Jin, Shoukun Han & Jingping Rao

Fruit softening is mainly associated with cell wall structural modifications, and members of the xyloglucan endotransglucosylase/hydrolase (XTH) family are key enzymes involved in cleaving and re-joining xyloglucan in the cell wall. In this work, we isolated a new *XTH* gene, *DkXTH8*, from persimmon fruit. Transcriptional profiling revealed that *DkXTH8* peaked during dramatic fruit softening, and expression of *DkXTH8* was stimulated by propylene and abscisic acid but suppressed by gibberellic acid and 1-MCP. Transient expression assays in onion epidermal cells indicated direct localization of DkXTH8 to the cell wall via its signal peptide. When expressed *in vitro*, the recombinant DkXTH8 protein exhibited strict xyloglucan endotransglycosylase activity, whereas no xyloglucan endohydrolase activity was observed. Furthermore, overexpression of *DkXTH8* resulted in increased leaf senescence coupled with higher electrolyte leakage in *Arabidopsis* and faster fruit ripening and softening rates in tomato. Most importantly, transgenic plants overexpressing *DkXTH8* displayed more irregular and twisted cells due to cell wall restructuring, resulting in wider interstitial spaces with less compact cells. We suggest that *DkXTH8* expression causes cells to be easily destroyed, increases membrane permeability and cell peroxidation, and accelerates leaf senescence and fruit softening in transgenic plants.

Fruit softening occurs primarily through modifications to the cell wall as the result of cell wall polymer degradation catalyzed by diverse enzymes such as cellulase, polygalacturonase,  $\beta$ -galactosidase, pectate lyase, and xyloglucan endotransglycosylase/hydrolase (XTH)<sup>1–3</sup>. Indeed, the depolymerization and solubilization of pectic and hemicellulosic polysaccharides in the cell wall have been demonstrated to be the major processes in fruit softening<sup>4</sup>. Xyloglucan, the major hemicellulose in the primary cell wall of dicotyledonous plants, comprises a network with cellulose microfibrils to provide strength to the cell wall<sup>5,6</sup>, with xyloglucan endotransglucosylases/hydrolases (XTHs) functioning in xyloglucan metabolism through xyloglucan endotransglycosylase (XET) and/or xyloglucan endohydrolase (XEH) activities<sup>7,8</sup>. XET activity results in the transfer of one xyloglucan molecule to another, whereas XEH activity hydrolyzes one xyloglucan molecule from the polymer<sup>9,10</sup>.

Enzymes exhibiting XTH activity belong to a multigene family<sup>11</sup> with at least 33 genes isolated from *Arabidopsis thaliana*<sup>12</sup> and 25 genes from tomato<sup>8</sup>. Expression of *XTH* genes is regulated by developmental and environmental stimuli<sup>13</sup>, such as darkness, touch, cold/heat-shock<sup>14,15</sup>, and by many hormones, such as ethylene<sup>16</sup>, abscisic acid (ABA)<sup>6</sup>, gibberellic acid (GA<sub>3</sub>)<sup>17</sup>, and auxins<sup>18</sup>.

XTHs have generally been thought to play important roles in fruit ripening and softening through activities that loosen the cell wall and break down the cellulose-xyloglucan matrix<sup>19–22</sup>. XET activity was found to peak

College of Horticulture, Northwest A&F University, Yangling, 712100, Shaanxi, China. \*These authors contributed equally to this work. Correspondence and requests for materials should be addressed to J.R. (email: raojingpingxn@163.com)



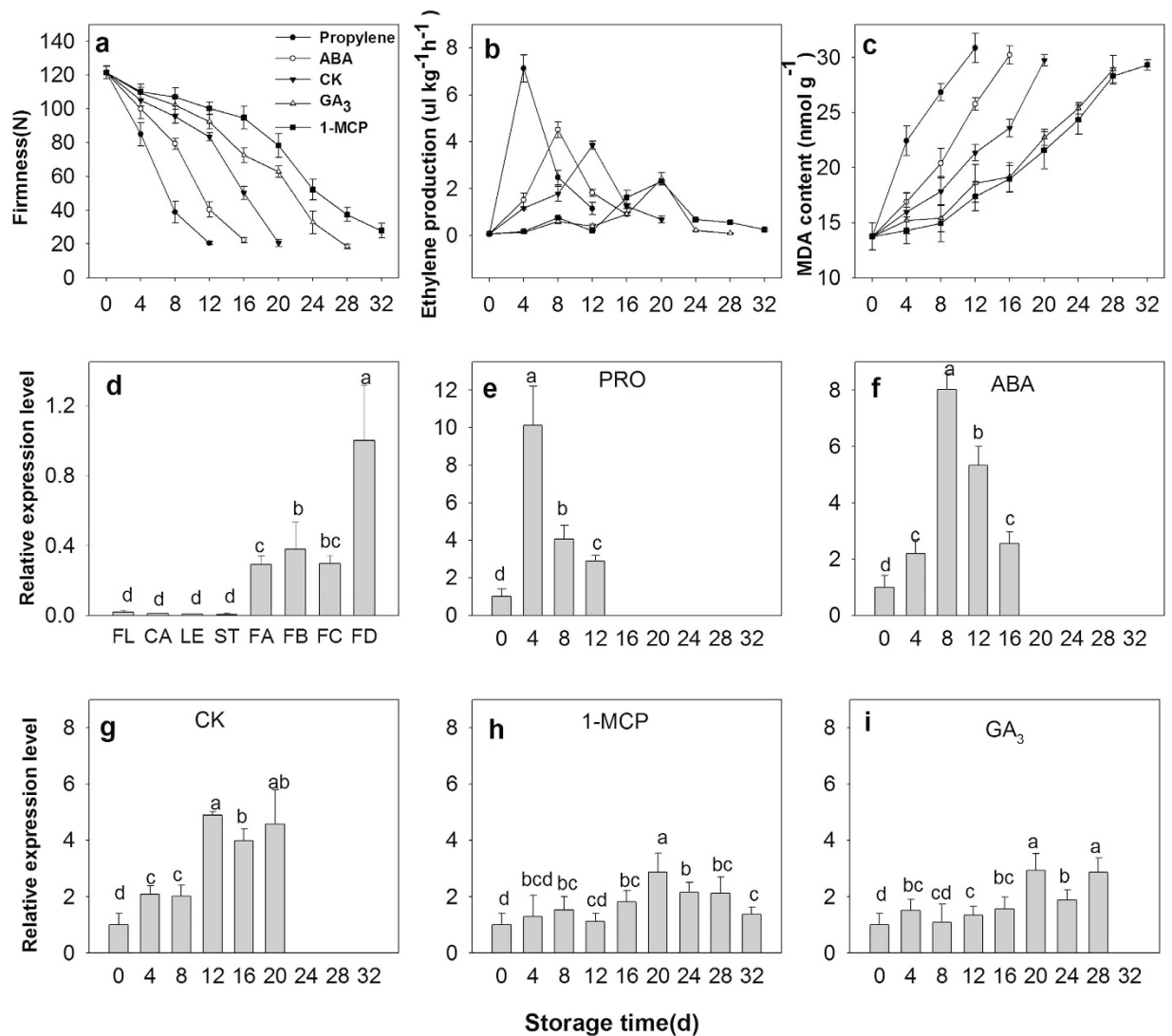


**Figure 2. Physiological characterization of persimmon and expression pattern of *DkXTH8*.** Firmness (a), ethylene production (b) and MDA content (c) of persimmon fruits during storage. ‘Propylene’ ‘1-MCP’ ‘ABA’ and ‘GA<sub>3</sub>’ indicated Fuping Jianshi fruit treated with propylene (5000 μl L<sup>-1</sup>, 24 h), 1-MCP (500 nL L<sup>-1</sup>, 24 h), ABA (50 mg L<sup>-1</sup>, 2 min) and GA<sub>3</sub> (60 mg L<sup>-1</sup>, 2 min), respectively. The fruit without any treatment was served as the ‘CK’. (d) Expression pattern of *DkXTH8* in various tissues of persimmon. ‘FL’ ‘CA’ ‘LE’ and ‘ST’ are indicated the flowers, calyces, leaves and stems, respectively. ‘FA’ ‘FB’ ‘FC’ and ‘FD’ are indicated fruits harvested at 20, 60, 100 and 140 days after full bloom, respectively. Expression of *DkXTH8* at ‘FD’ was used as the control with a nominal value of 1. Expression pattern of *DkXTH8* in ‘Propylene’ (e), ‘ABA’ (f), ‘CK’ (g), ‘1-MCP’ (h) and ‘GA<sub>3</sub>’ (i) persimmon fruits. Expression of *DkXTH8* at 0 day was used as the control with a nominal value of 1. Vertical bars indicate the standard error of three replicate assays. Columns with different letters at each time point are significantly different (LSD,  $P < 0.05$ ).

16 enzymes, DkXTHs have two conserved central domains, and two cysteine residues are located in the C terminal region, suggesting that DkXTH8 shares common features with XTHs from other plants.

**Physiological characterization during persimmon fruit storage.** To analyze postharvest softening and senescence, uniform persimmon fruits free from visible defects and with 70–80% surface yellow coloration were harvested. After treatment (propylene, ABA, GA<sub>3</sub> and 1-MCP), fruits were stored at room temperature and randomly collected every 4 days for physiological characterization. When testing firmness (Fig. 2a), the control fruit (“Fuping jianshi” fruit without any treatment, CK) were obviously softened at 12 days after harvest; firmness was 122 N at harvest time, declining to 21 N on day 20. However, the firmness of the fruits treated with propylene and ABA (“Fuping jianshi” fruit treated with propylene and ABA, respectively) decreased more quickly than that of the CK fruit, showing a higher rate of softening. In detail, the CK fruit firmness was 75% and 51% firmer than the propylene and ABA fruits at 12 days of storage, respectively. In contrast, the firmness of the GA<sub>3</sub> and 1-MCP fruits (“Fuping jianshi” fruits treated with GA<sub>3</sub> and 1-MCP, respectively) declined more slowly than that of the CK

fruit, showing a lower rate of softening. Specifically, the GA<sub>3</sub> and 1-MCP fruit firmness was 67% and 74% firmer than the CK fruit at 20 days of storage, respectively.

The ethylene production of the fruits was measured during storage (Fig. 2b). Ethylene production was stimulated by propylene and ABA, and the maximal values in the propylene- (4 days) and ABA-treated fruits (8 days) was 46% and 16% higher than that in the CK fruit (12 days), respectively. Conversely, the ethylene production was inhibited in GA<sub>3</sub> and 1-MCP fruits. In detail, the maximal ethylene production in GA<sub>3</sub> and 1-MCP fruit (20 days) was only 63% and 61% of that in CK fruit, respectively.

After harvest, the malonaldehyde (MDA) content rose consistently in all of the tested fruits (Fig. 2c). In CK fruits, the MDA content was 13.8 nmol g<sup>-1</sup> at harvest time and increased up to 29.8 nmol g<sup>-1</sup> at the end of storage. Whereas, the MDA contents of the propylene and ABA fruits remained higher than that of the CK fruit, revealing accelerated MDA accumulation in the treated fruits. In contrast, the MDA content of the fruits treated with GA<sub>3</sub> and 1-MCP remained at low levels, and the value at 20 days was only 76% and 72% of that in the CK fruit, respectively.

**Expression of *DkXTH8* in different persimmon tissues and during fruit storage.** Leaves, flowers, calyces, stems and fruits were analyzed to examine the expression pattern of *DkXTH8* in different tissues (Fig. 2d). *DkXTH8* transcripts were notably detectable in fruits, though very little expression was found in other tissues. Moreover, fruits collected at 140 days after full bloom shown evidently higher *DkXTH8* expression levels than fruits harvested at 20, 60 or 100 days after full bloom.

To analyze the association of *DkXTH8* with fruit softening, the levels of expression were measured in propylene-, ABA-, GA<sub>3</sub>- and 1-MCP-treated fruits (Fig. 2e–i). After harvest, *DkXTH8* transcripts increased rapidly, peaking at 12 days after storage in CK fruit. Moreover, a similar expression pattern was observed in the propylene and ABA fruits, peaking at 4 or 8 days after storage, respectively. The expression pattern of *DkXTH8* appeared parallel to ethylene production, and both of them peaked during dramatic fruit softening. Additionally, the maximal values of *DkXTH8* expression in the propylene- and ABA-treated fruits were 52% and 39% higher than that in the CK fruit, revealing the synergistic effect of propylene and ABA on *DkXTH8* expression. In contrast, the GA<sub>3</sub> and 1-MCP fruits exhibited lower levels of *DkXTH8* expression, with respective maximal values of only 60% and 58% of CK fruit.

**Direct localization of *DkXTH8* to the cell wall via its signal peptide.** The ORF of *DkXTH8* (*DkXTH8*Full), the signal peptide of *DkXTH8* (*DkXTH8*-SP), and the ORF sequence of *DkXTH8* without the signal peptide (*DkXTH8*-Int) were amplified. A schematic diagram of the vector construction is shown in Fig. 3a. The subcellular localization of *DkXTH8* was analyzed by bombarding plasmids into onion epidermal cells. Three types of results were observed: “Fluorescent”, “Bright” and “Merged” (see Fig. 3b). *DkXTH8*Full protein was detected in cell walls by monitoring the plasmolyzed and non-plasmolyzed cells; this was different from the GFP control, for which protein was found throughout the cell. In control plasmolyzed cells, the fluorescence protein was obviously found in both the cell wall and plasma membrane, however, *DkXTH8*Full protein was only observed in cell walls. Besides, *DkXTH8*-SP protein was specifically localized to the cell wall. Nevertheless, in the absence of the signal peptide, *DkXTH8*-Int was localized throughout the cell, suggesting that its N-terminal signal peptide targets *DkXTH8* to the cell wall.

**The recombinant *DkXTH8* protein possesses strict XET activity.** The recombinant *DkXTH8* protein (*DkXTH8*-RP) was expressed in bacteria to investigate its enzymatic properties. To promote correct protein folding, the protein was induced at low-speed shaking and at a low temperature. However, only a small proportion of the protein was soluble, with most of the recombinant protein present in the insoluble fraction (Fig. 4a). After concentration and purification using a Ni-NTA resin column, the soluble recombinant protein was used for assessing enzyme activity. Obvious XET activity was detected for *DkXTH8*-RP in comparison with the blank control, suggesting that the purified recombinant *DkXTH8* protein was an active enzyme (Fig. 4b). The XEH activity of *DkXTH8*-RP was also measured by a viscometric assay using *Trichoderma reesei* cellulose as a positive control. Unlike *Trichoderma reesei* cellulose, which could reduce the viscosity of xyloglucan via hydrolytic action, *DkXTH8*-RP did not cause any evident decrease in viscosity of xyloglucan after a set reaction time. These results indicate that *DkXTH8*-RP possesses strict XET activity, with no XEH activity.

To examine the pH profile of *DkXTH8*-RP, XET activity was tested over the pH range of 3–8 (Fig. 4c). A bell-shaped pH profile was found and the XET activity declined sharply when the pH decreased from 5 to 4, as a common feature of XET enzymes<sup>32</sup>. The XET activity of *DkXTH8*-RP was also tested over the temperature range from 5 to 60 °C, and the optimum temperature for the enzyme was found to be in the range 30–40 °C (Fig. 4d).

**Overexpression of *DkXTH8* in *Arabidopsis* promotes dark-induced leaf senescence.** To verify whether *DkXTH8* is involved in plant senescence, transgenic *Arabidopsis* lines (AL1, AL2, AL3) overexpressing *DkXTH8* were generated (Fig. S1b). After stored in the dark for four days, detached leaves of transgenic *Arabidopsis* became more visibly yellow than the leaves of wild type (WT, Fig. 5a). Compared with the control, the chlorophyll content declined in both WT and transgenic *Arabidopsis* leaves after storage in the dark. However, the transgenic *Arabidopsis* leaves contained less chlorophyll than WT (Fig. 5b), suggesting accelerated senescence in *DkXTH8*-overexpressing *Arabidopsis*. Furthermore, the MDA content and electrolyte leakage were measured in detached leaves to indicate the degree of cell peroxidation (Fig. 5c,d). The transgenic *Arabidopsis* leaves showed higher levels of electrolyte leakage and MDA content than WT, indicating more lipid peroxidation in the transgenic plant cells. Two senescence associated genes, *AtSAG12* and *AtSAG13*, were induced rapidly in dark stored leaves (Fig. 5e,f). While, both *AtSAG12* and *AtSAG13* exhibited higher expression levels in transgenic plants than that in WT, indicating critical leaf senescence in *DkXTH8*-overexpressing *Arabidopsis*.



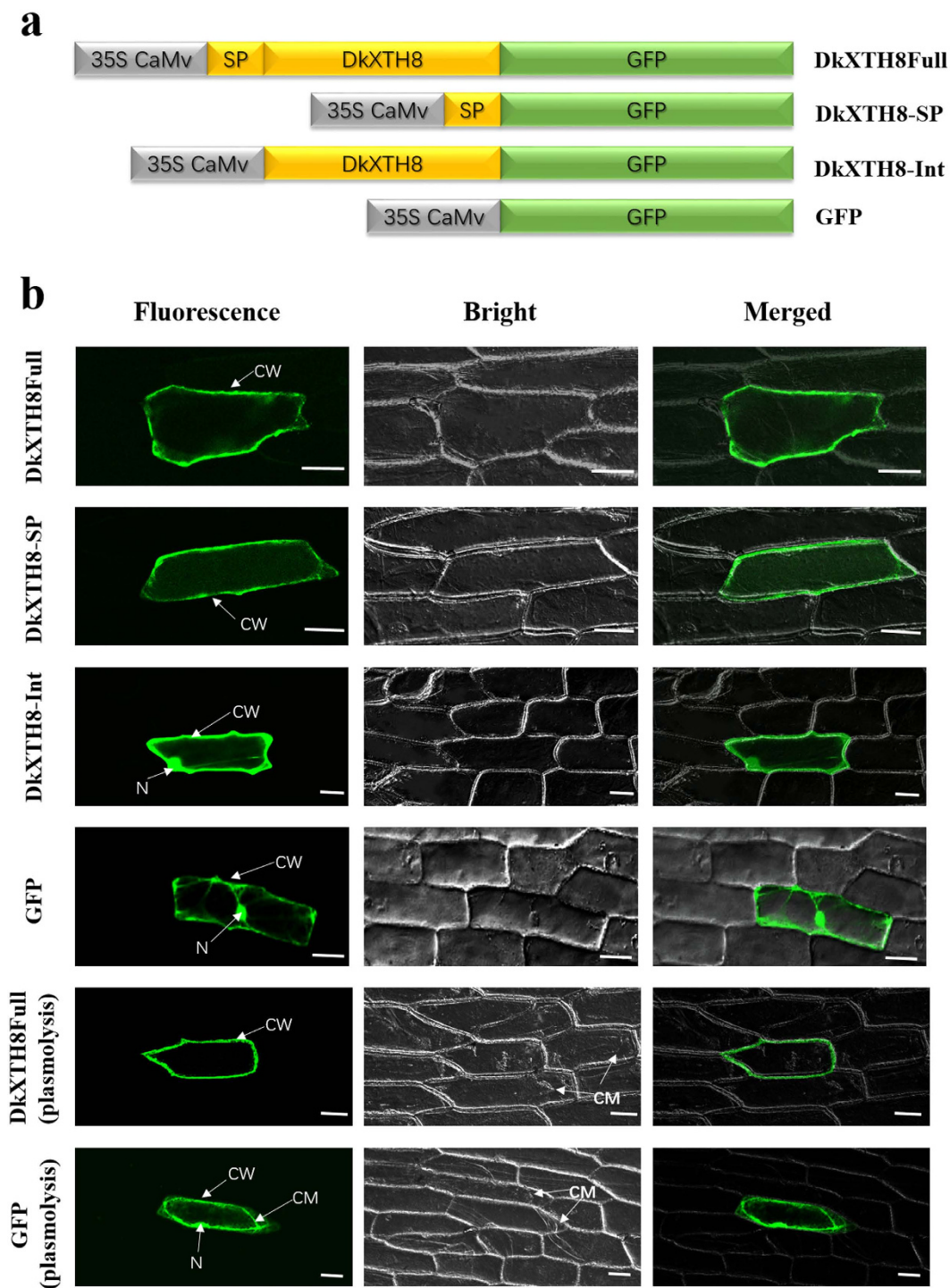


**Figure 3. Subcellular localization of DkXTH8.** (a) Diagram of DkXTH8 constructs fused to GFP. (b) “Fluorescent”, “Bright” and “Merged” images of subcellular localization of DkXTH8 and GFP control. Plasmolysis was induced by 400 mM sucrose. CW, cell wall; N, nucleus; CM, cell membrane. Scale bar = 50  $\mu$ m.

**Overexpression of *DkXTH8* in tomato promotes fruit ripening and softening.** *DkXTH8*-transgenic tomato lines (TL1, TL2, TL3) were generated to explore whether *DkXTH8* is related to fruit ripening and softening (Fig. S1c). Tomato fruits were collected at the mature green stage and stored at room temperature. Samples were randomly collected every 3 days, as shown in Fig. 6a. After harvesting, the fruits began to turn yellow and then red; however, the transgenic tomato fruits exhibited accelerated color change compared with the WT fruits. As a representation of color,  $L^*$ ,  $a^*$  and  $a^*/b^*$  values were measured to indicate tomato fruit maturity (Fig. 6b–d). In the WT fruits, the level of  $L^*$  declined constantly during storage. A marked decline was detected from 6 to 9 days, at which time the fruit turned from green to yellow. In contrast, the three transgenic tomato lines displayed

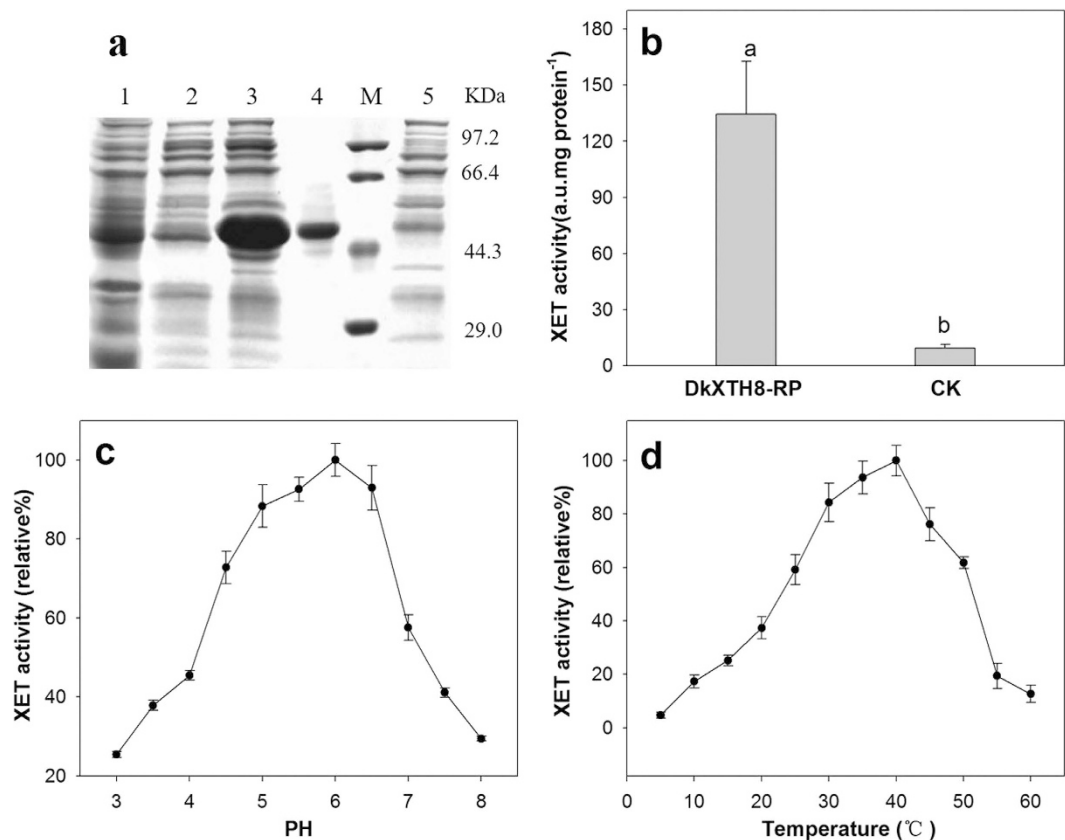


**Figure 4. Expression and activity of recombinant DkXTH8 proteins.** (a) Proteins were separated on SDS-polyacrylamide gels and stained with Coomassie Blue. Lane 1, total soluble protein (DkXTH8); lane 2, unbound protein; lane 3, total insoluble protein (DkXTH8); lane 4, purified protein (DkXTH8); M, protein marks (Takara, Dalian, China); and lane 5, pET-32a control protein. (b) *In vitro* XET assay of recombinant DkXTH8 proteins. The XET assay was performed by colorimetric method as described in Section 4.7. The empty vector pET-32a was used as the control. (c) The pH-rate profile of recombinant DkXTH8 proteins. Vertical bars indicate standard errors of three replicates. (d) The temperature profile of recombinant DkXTH8 proteins. Vertical bars indicate standard errors of three replicates.

a faster decrease in  $L^*$ , indicating rapid color change. Similarly, the values of  $a^*$  and  $a^*/b^*$  increased after storage though more rapidly in the transgenic fruits than in the WT fruits. The values of  $a^*$  and  $a^*/b^*$  were 76–81% and 71–77% higher, respectively, in the transgenic fruits than in the WT fruits after 9 days of storage.

When evaluating firmness, the transgenic fruits decreased faster than WT (Fig. 6e), with the firmness of the transgenic fruits only 75–88% and 54–63% of that in WT at 9 and 12 days, respectively. In addition, the maximal values of ethylene production by the transgenic fruits were higher than that in WT, and the peak appeared three days earlier (Fig. 6f). Moreover, the MDA content rose constantly after the fruits were harvested, 12–16% higher in the transgenic fruits than that in WT at the end of storage (Fig. 6g).

Ethylene synthesis related genes were also assessed to indicate the degree of fruit ripening and softening in WT and *DkXTH8*-overexpressed tomatoes. Both *ACS* and *ACO* genes were up regulated during fruit storage, however, relative higher expression levels were found in transgenic tomato fruits (Fig. 6h–j). In *DkXTH8*-overexpressed fruits, the expression levels of *LeACS2* and *LeACO1* were 39–58% and 21–38% higher than that in WT, respectively (6 days after storage,  $p < 0.05$ ).

**Microscopic observation of WT and *DkXTH8*-transgenic plants.** To assess whether the differences in the leaf senescence rate and fruit softening were due to changes in cell wall structure, the microscopic structures of WT and *DkXTH8*-transgenic plants were compared. The stems and fifth–sixth leaves of *Arabidopsis* plants were collected at four weeks after sowing. Compared with WT, the leaf sections of the transgenic *Arabidopsis* plants showed more irregularity, especially in the lower and upper epidermis layers, exhibiting a winding shape (Fig. 7a,b). Similar observations were found in stem sections. A longitudinal section of the stem from the *DkXTH8*-transgenic plants exhibited an irregular shape with a slightly wave-like border in the epidermis (Fig. 7c,d). Similarly, the epidermis and cortex contained more irregularly shaped cells in stem cross sections from the transgenic *Arabidopsis* plants (Fig. 7e,f). In particular, the cells of the xylem were rounded and smooth in WT but showed an angular and irregular shape in the transgenic plants.

Microscopic observations of WT and *DkXTH8*-transgenic tomato were carried out using fruits stored for 0, 9 and 18 days. At harvest time (0 days), the cells from WT fruits were rounded and smooth with a uniform size (Fig. 8a,b). In contrast, the cells from the transgenic fruits were more angular and irregular with multiple

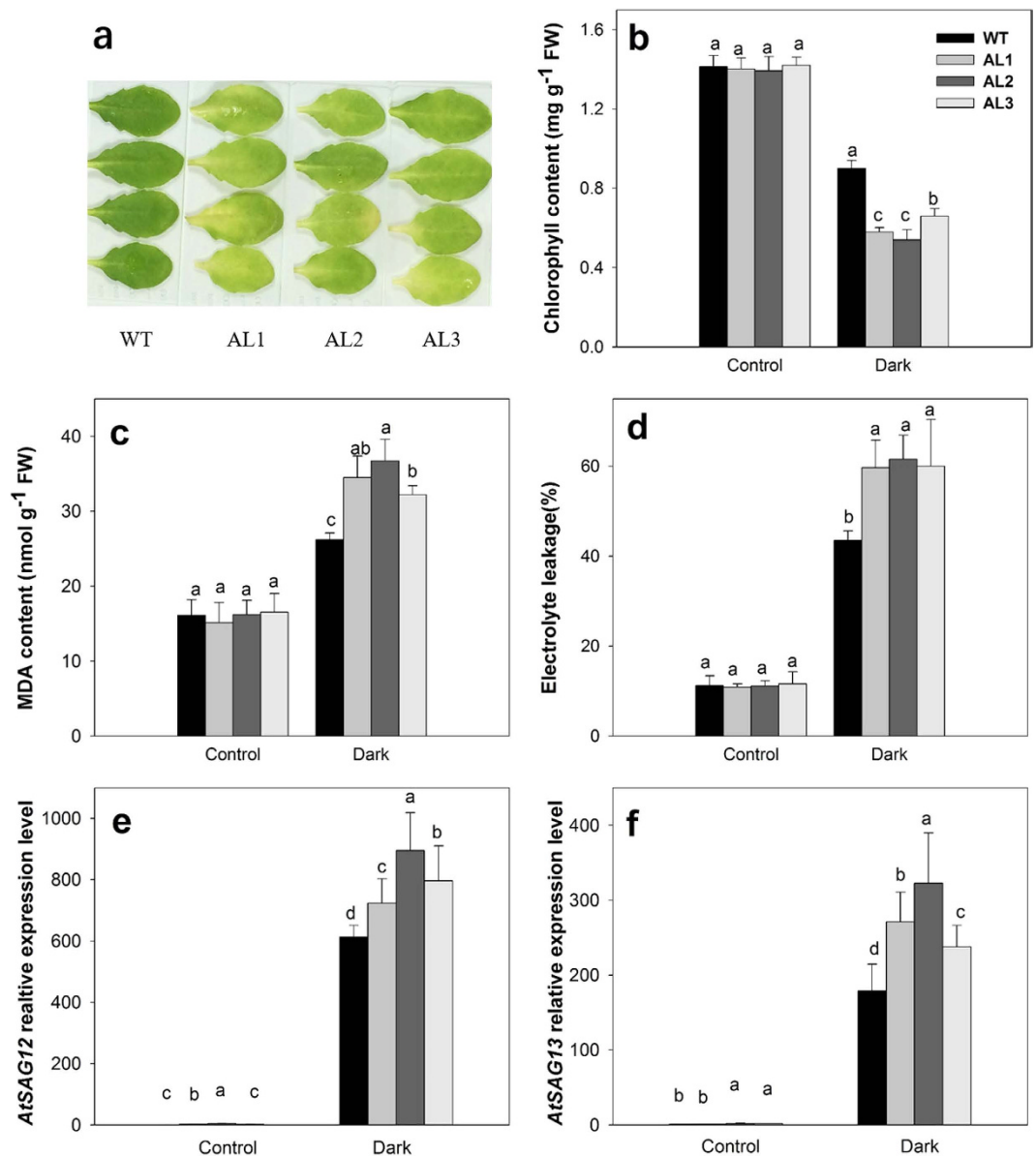


**Figure 5.** Dark-induced leaves senescence of WT and *DkXTH8*-overexpressing *Arabidopsis*. (a) Visual appearance of detached leaves of WT and *DkXTH8*-overexpressing *Arabidopsis* after four days in dark. (b) Chlorophyll content. (c) MDA content. (d) Electrolyte leakage. (e) Relative expression level of *AtSAG12* gene in WT and *DkXTH8*-transgenic *Arabidopsis* leaves. (f) Relative expression level of *AtSAG13* gene in WT and *DkXTH8*-transgenic *Arabidopsis* leaves. Detached leaves stored under growth conditions served as the control. Vertical bars indicate the standard error of three replicate assays. Columns with different letters at each time point are significantly different (LSD,  $P < 0.05$ ).

sizes, resulting in a wider interstitial space and less compact cells (Fig. 8c,d). At the middle of the storage period (9 days), the majority of cells from the WT fruits retained their integrity, and only a few cells were degraded (Fig. 8e,f). However, more than half of the cells from the transgenic fruits were degraded, suggesting a higher rate of fruit softening (Fig. 8g,h). At the end of storage (18 days), nearly all cells from the transgenic fruits were degraded (Fig. 8k,l). Although most of the cells from the WT fruits were destroyed, the third-fourth layer cells under the peel retained integrity (Fig. 8i,j).

## Discussion

Previous works have reported that XTHs are encoded by a large multigene family<sup>9,10</sup>. Individual XTHs exhibit multiple expression patterns and diverse responses to hormonal or environmental stimuli, which may account for their unique roles in fruit<sup>33,34</sup>. In previous studies, we isolated seven *XTH* genes from persimmon, and all of these genes were found to play important roles in fruit development, ripening or softening<sup>6,27</sup>. In the present study, a new *XTH* gene from persimmon was identified: *DkXTH8*. Phylogenetic analysis revealed that *DkXTH8* belongs to group II (Fig. 1a), different from *PttXET16A* and *TmNXG1*, strict XET and XEH enzymes, respectively<sup>30,31</sup>.

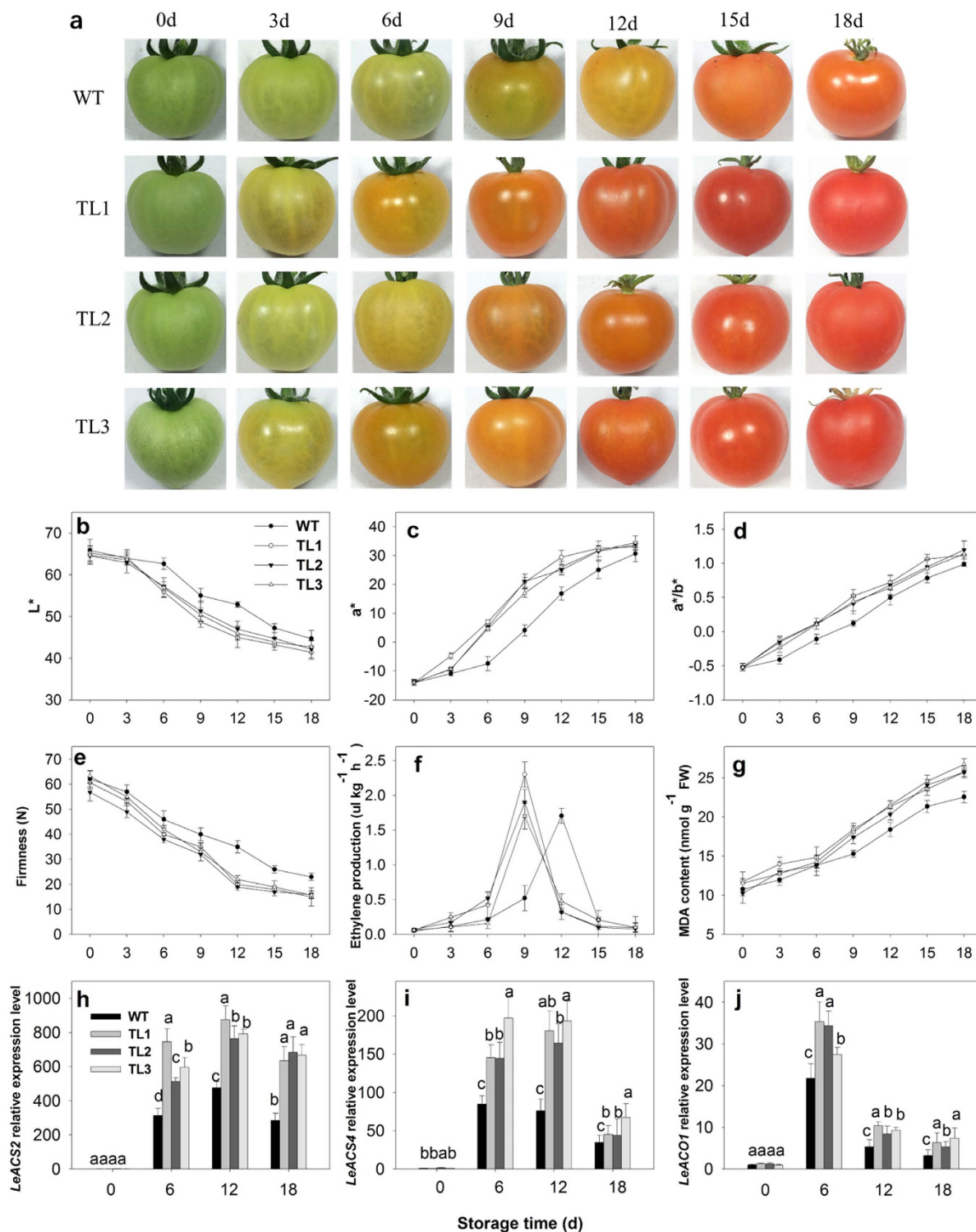


**Figure 6. Phenotype and physiological parameters of WT and *DkXTH8*-overexpressing tomato.** (a) Fruit phenotype. Tomato fruits of WT and *DkXTH8*-transgenic lines were collected at the mature green period and stored at room temperature. Samples were randomly collected every 3 days. (b–d) Changes in  $L^*$ ,  $a^*$  and  $a^*/b^*$  colour parameters of tomato fruit. (e–g) Changes in firmness, ethylene production and MDA contents of fruit. (h–j) Relative expression levels of *LeACS2*, *LeACS4* and *LeACO1* genes in fruit. Vertical bars indicate the standard error of three replicate assays.

Sequence analysis indicated that *DkXTH8* shares 50–70% homology with *DkXTH1–7* and contains the conserved regions of glycosyl hydrolase family 16 genes (Fig. 1b), indicating that this new gene possesses the common structural features of XTHs<sup>11</sup>.



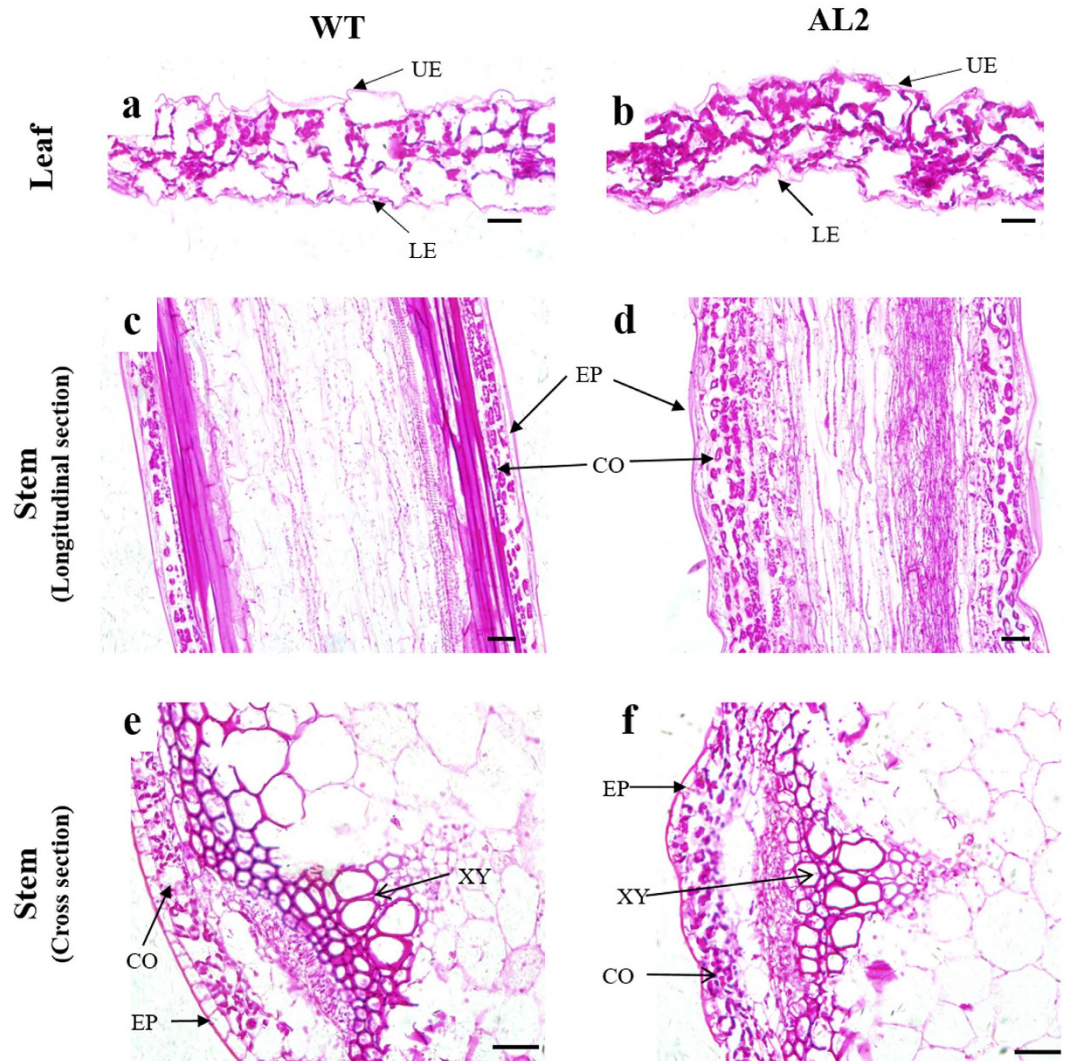


**Figure 7.** Microscopic observation of WT and *DkXTH8*-overexpressing *Arabidopsis*. Leaf section of WT (a) and *DkXTH8*-transgenic *Arabidopsis* (b). Longitudinal section of the stem from WT (c) and *DkXTH8*-transgenic *Arabidopsis* (d). Cross section of the stem from WT (e) and *DkXTH8*-transgenic *Arabidopsis* (f). Scale bar = 20  $\mu$ m. UE, upper epidermis; LE, lower epidermis; EP, epidermis; CO, cortex; XY, xylem.

Propylene and ABA treatments of persimmon fruit resulted in a higher climacteric ethylene peak, lower firmness and an increased MDA content compared to CK fruit (Fig. 2a–c). More importantly, expression level of *DkXTH8* was effectively stimulated and appeared to parallel the fruit softening rate (Fig. 2e–i). This feature is consistent with previous work of rose *RbXTH1* and *RbXTH2*, which play important roles in senescence<sup>16</sup>. In contrast, exogenous GA<sub>3</sub> and 1-MCP inhibited ethylene production and effectively suppressed *DkXTH8* expression, which appeared to result in higher firmness of persimmon fruit. Similar results have been reported for papaya *CTR1*<sup>35</sup>, cherimoya *AcXET1*-3<sup>36</sup>, and apple *MdXTH10* and *MdXTH11*<sup>22</sup>, which have been demonstrated to be involved in fruit softening. Interestingly, *DkXTH8* was notably detected in mature persimmon fruit but scarcely in other tissues or unripe fruit (Fig. 2d). Overall, the results suggest that *DkXTH8* is a fruit ripening-specific gene that most likely operates in conjunction with ethylene during postharvest fruit softening.

Isoenzymes of XTHs possess distinct enzymatic properties<sup>37,38</sup>, with specialized functions in cell wall modification<sup>10,39</sup>. In persimmon, *DkXTH1* and *DkXTH2* exhibit different affinities for small acceptor molecules, and the former might participate in cell wall assembly, whereas the latter is likely involved in cell wall restructuring<sup>27</sup>. The kinetic properties of the recombinant *DkXTH8* protein (*DkXTH8*-RP) were investigated, with *DkXTH8*-RP showing significant XET activity without any detectable XEH activity (Fig. 4b). These results are similar to the reports of recombinant *SlXTH5* protein from tomato<sup>40,8</sup> and *AtXTH14* and *AtXTH26* from *Arabidopsis*<sup>41</sup>. *DkXTH8*-RP exhibited a bell-shaped pH profile (Fig. 4c), and the optimum temperature for the enzyme was in the range 30–40 °C (Fig. 4d), as a common feature of XET enzymes<sup>42</sup>. In addition, the *DkXTH8* protein was directly localized to the cell wall via its signal peptide (Fig. 3). *ZmXTH1*, a cell wall-bound maize protein, has been shown to affect the cell wall structure and composition in transgenic *Arabidopsis*<sup>43</sup>. The *PeXTH* gene from *Populus euphratica* caused anatomical and physiological alterations in transgenic tobacco and was localized to the

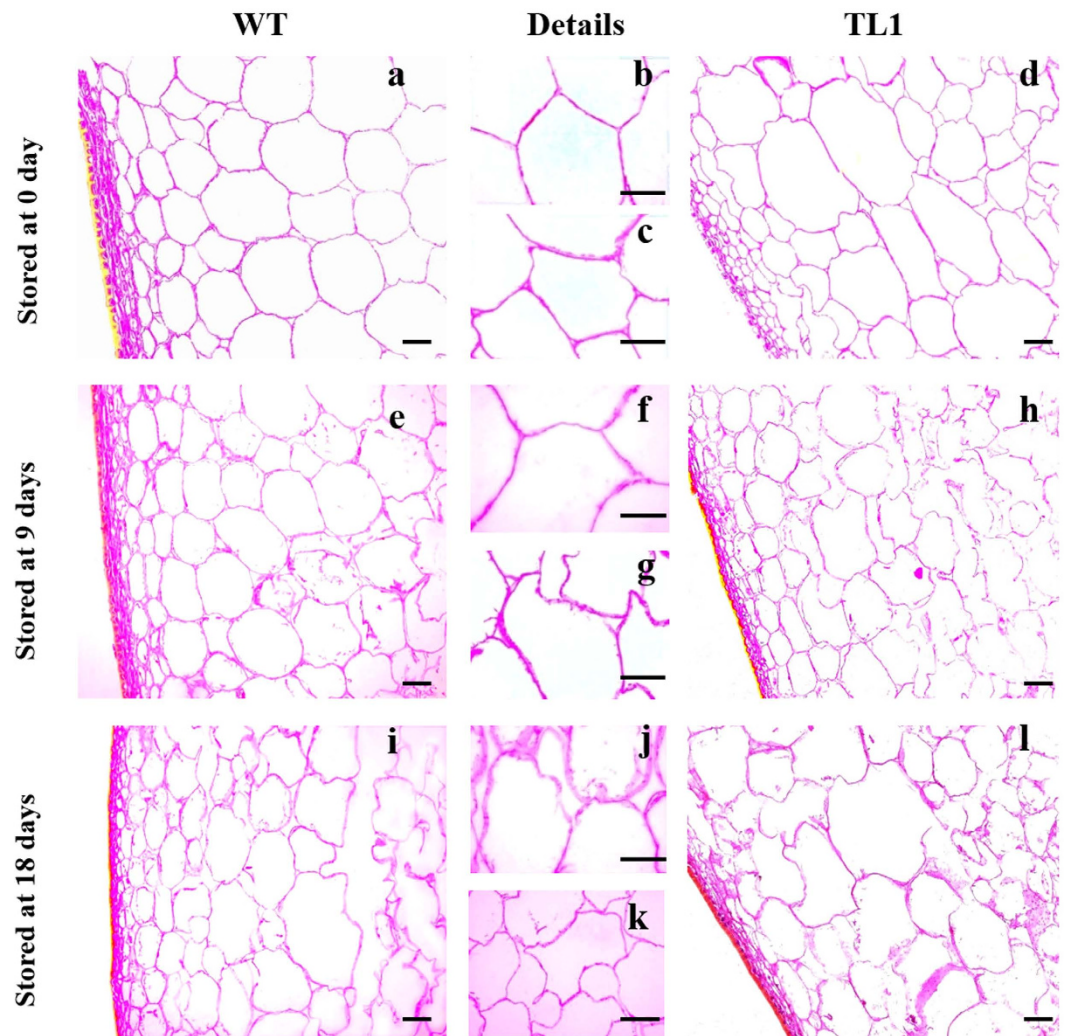


**Figure 8. Microscopic observation of WT and *DkXTH8*-overexpressing tomato.** Microscopic observation of WT (a,b) and *DkXTH8*-overexpressing tomato fruit (c,d) stored at 0 day; Microscopic observation of WT (e,f) and *DkXTH8*-overexpressing tomato fruit (g,h) stored at 9 days; Microscopic observation of WT (i,j) and *DkXTH8*-overexpressing tomato fruit (k,l) stored at 18 days. Scale bar = 50  $\mu$ m.

endoplasmic reticulum and cell wall<sup>44</sup>. Therefore, *DkXTH8* is suggested to act as an XET enzyme that is directly localized to the cell wall and is involved in cell wall modification.

The relationship between *DkXTH8* and leaf senescence was investigated in transgenic *Arabidopsis*. Leaf senescence was detected based on the loss of chlorophyll<sup>45</sup>, which was accompanied by an increase in lipid peroxidation and membrane permeability<sup>46</sup>. In our study, leaf senescence was promoted in *DkXTH8*-transgenic *Arabidopsis*, coupled with higher chlorophyll degradation, electrolyte leakage and MDA content (Fig. 5). Meanwhile, both *AtSAG12* and *AtSAG13* shown higher expression levels in transgenic plants than that in WT, which expression were strictly associated with senescence. Wagstaff *et al.* suggested that decreased expression of lettuce *LsXTH* altered the leaf biophysical structure and increased the leaf strength, leading to an extended shelf-life of transgenic plants<sup>47</sup>. Both the leaf and stem cells of *DkXTH8*-transgenic *Arabidopsis* showed more irregular and twisted shapes, resulting in a wider interstitial space and less compact cells compared with WT (Fig. 7). Similar results have been reported in maize: *ZmXTH1* was demonstrated to affect cell wall structure in transgenic *Arabidopsis*, with a wider middle lamella region that resulted in a widening of the space between cells<sup>43</sup>. These results raise the possibility that overexpression of *DkXTH8* affected the structure of the cell wall, resulting in a wider interstitial space and less compact cells. Notably, these changes in shape caused the cells to be easily destroyed and also increased lipid peroxidation and membrane permeability, exacerbating leaf senescence.

To confirm whether *DkXTH8* is involved in fruit ripening and softening, further verification was performed in *DkXTH8*-transgenic tomato. Compared to WT, the *DkXTH8*-transgenic tomato fruit exhibited accelerated color change, decreased firmness and increased MDA content (Fig. 6). The expression levels of *LeACS2*, *LeACS4* and *LeACO1* displayed higher values in transgenic fruits accompanied by an earlier and higher ethylene peak. This is the first direct genetic evidence for the promotion of fruit ripening and softening by XTHs. Overexpression of tomato *SIXTH1* was demonstrated to reduce the softening of transgenic fruit, and the author suggested that XET



was involved in maintaining the structural integrity of the cell wall<sup>26</sup>. However, *SIXTH1* was transiently detected at high levels during the early stage of fruit development, with little expression during fruit ripening or softening in tomato<sup>24,25</sup>. *DkXTH1*, which was found to be largely expressed in fast-growing persimmon fruit, was demonstrated to contain fruit firmness by participating in cell wall assembly<sup>27</sup>. While, *DkXTH2*, a gene expressed mainly in ripening persimmon fruit, likely promotes fruit softening via restructuring of the cell wall<sup>27</sup>. Thus, we suggest that the fruit ripening-specific gene *DkXTH8* may promote transgenic tomato fruit softening through involvement in cell wall restructuring.

In agreement with the results in *Arabidopsis*, *DkXTH8*-transgenic tomato fruit exhibited more irregular and twisted cells, leading to wider interstitial spaces and less compact cells compared with WT (Fig. 8). Furthermore, accelerated cell degradation was found in the postharvest transgenic fruit, resulting in a higher degree of fruit softening. Altogether, the results suggest that overexpression of *DkXTH8* altered cell shape in the transgenic fruit by acting in cell wall restructuring, which resulted in wider interstitial spaces and less compact cells. These changes in shape caused the cells to be easily destroyed, intensifying fruit softening.

In conclusion, a new xyloglucan endotransglucosylase/hydrolase, *DkXTH8*, was identified from persimmon. This gene presented the highest expression levels during fruit ripening and softening. The recombinant *DkXTH8* protein showed strict XET activity and no XEH activity. Overexpression of *DkXTH8* caused more irregular and twisted cells, with wider interstitial spaces and less compact cells via its involvement in cell wall restructuring, which resulted in accelerated leaf senescence in *Arabidopsis* and fruit softening in tomato.

## Methods

**Plant materials and treatments.** Persimmon materials were obtained from a commercial orchard in Fuping County, Shaanxi Province, China. The propylene treatment was performed by placing fruits in a 360-L chamber and exposing them to 5000  $\mu\text{L L}^{-1}$  propylene for 24 h. The 1-MCP treatment was performed by exposing fruits to 500  $\text{nL L}^{-1}$  1-MCP (EthylBloc<sup>®</sup>, Dow Chemical Co., Shanghai, China, a.i. 0.14%) for 24 h. The GA<sub>3</sub> treatment was carried out by immersing fruits in 60  $\text{mg L}^{-1}$  GA<sub>3</sub> for 2 min and the ABA treatment by immersing fruits in 50  $\text{mg L}^{-1}$  ABA for 2 min. Untreated fruits served as the control ('CK'). After treatment, each group was divided randomly into three subgroups, and all fruits were stored at 25  $\pm$  1 °C.

For *DkXTH8* functional analyses, *Arabidopsis thaliana* ecotype 'Columbia' and *Solanum lycopersicum* Mill. cultivar 'Micro-Tom' were used.

**RNA extraction and isolation of the full-length *DkXTH8* cDNA.** Total RNA was isolated from frozen persimmon tissues using the hot borate method<sup>27</sup>, and TransZol Up Plus RNA Kit (Transgen Biotech, Beijing, China) was used to extract total RNA from *Arabidopsis* and tomato. First-strand cDNA was obtained using a PrimeScript RT Reagent Kit with gDNA Eraser (TaKaRa, Dalian, Japan). Based on the degenerate primers designed by Zhu *et al.*<sup>6</sup>, a new conserved *XTH* gene region was amplified using material from persimmon fruit as a template. Subsequently, 3'- and 5'-rapid amplification of cDNA ends polymerase chain reactions (PCR) were performed as described in Han *et al.*<sup>27</sup>, and the full-length cDNA of *XTH* was then amplified based on the 3'-end and 5'-end fragments. The primer sequences are listed in Table 1.

**Sequence analysis and bioinformatic methods.** The full-length *XTH* sequence was confirmed using the BLAST program in GenBank, and ORF Finder at NCBI (<http://www.ncbi.nlm.nih.gov/gorf/gorf.html>) was used for ORF and protein predictions. The PeptideMass program (<http://us.expasy.org/tools/peptidmass.html>) was employed to calculate the molecular weight and theoretical isoelectric point (*pI*) of the putative protein, and SignalP (<http://www.cbs.dtu.dk/services/SignalP/>) was used for N-terminal signal peptide prediction. The deduced amino acid sequences were initially aligned and compared using the DNAMAN program, and a phylogenetic tree was generated based on the Neighbor-Joining method (1000 bootstrap replicates) using MEGA 5.1 software.

**Fruit firmness, ethylene production and MDA content determination.** To measure fruit firmness, three small slices of skin were removed from 120° intervals around the equatorial axis of a fruit. A pressure tester equipped with a 5- or 1-mm diameter probe was used for persimmon and tomato fruits, respectively. For each time point, six fruits were tested for replications.

Six fruits from each treatment subgroup were placed in an airtight chamber for 1 h at room temperature, and 1 mL of gas was collected three times using a syringe. The ethylene concentration was then quantified using a GC-14A gas chromatograph (Shimadzu, Kyoto, Japan), as described by Zhu *et al.*<sup>6</sup> The respiration rate was measured using a CO<sub>2</sub> infrared gas analyzer (TEL7001; GE Telaire, CA, USA) according to Han *et al.*<sup>27</sup>.

The MDA content was measured and calculated according to Hou *et al.*<sup>28</sup>.

**Quantitative real-time (RT)- qPCR expression analysis.** First-strand cDNA was synthesized using the methods described above. RT-qPCR was then carried out using an iCycler iQ5 (Bio-Rad, Hercules, CA, USA) as described by Han *et al.*<sup>27</sup>. *DkACTIN*, *AtACTIN2* and *LeUBI3* were used as an internal control for persimmon, *Arabidopsis* and tomato, respectively. Standard curves were generated to ensure amplification efficiencies between the primers for the housekeeping genes and studied genes. The gene relative expression level was calculated using the comparative C<sub>T</sub> ( $2^{-\Delta\Delta C_T}$ ) method<sup>48</sup>. Three biological replicates were performed for all of the samples. The specific primer sequences used for qRT-PCR are listed in Table 1.

**Subcellular localization.** Subcellular localization of *DkXTH8* was investigated in onion epidermal cells with a biolistic PDS-1000/He particle delivery system (Bio-Rad), as described by Han *et al.*<sup>27</sup>. The ORF of *DkXTH8* (*DkXTH8*Full), the signal peptide of *DkXTH8* (*DkXTH8*-SP), and the ORF sequence of *DkXTH8* without the signal peptide (*DkXTH8*-Int) were amplified using the specific primers listed in Table 1. After confirmation, the

Gene name	Prime sequences (5'–3')	Purpose
<i>DkXTH8</i>	Outer: ATTCCGCCGCACCCATCTCA	5'RACE
	Inner: TCATCGGCTGGCGAAGGTAG	
	Outer: GAACGGGAGCAGCAGTTTC	3'RACE
	F: ACTGCTACTGCTGGCTTCATG	Full-length cDNA clone
	R: ATCTGATTCGCCCGCACCCATC	
	F: TCCTCCAACCTTAACCAGG	RT-qPCR
	R: ATCAATCTTGCCGAACAG	
	F: <u>GCTCTAGA</u> ATGGCGGCTTCTCCATATT	DkXTH8Full
	R: <u>GGGGTACC</u> TATATGGAGATTTAATTTGC	
	F: <u>GCTCTAGA</u> ATGGCGGCTTCTCCATATT	DkXTH8-SP
	R: <u>GGGGTACC</u> GGAGGAAGAAGAGGAAAGC	
	F: <u>GCTCTAGA</u> AACCTTAACCAGGATTTAA	DkXTH8-Int
	R: <u>GGGGTACC</u> TATATGGAGATTTAATTTGC	
	F: <u>CGGGATCC</u> AACCTTAACCAGGATTTT	Recombinant protein expression
	R: <u>CCCAAGCTT</u> TATATGGAGATTTAATTTGC	
F: <u>GCTCTAGA</u> ATGGCGGCTTCTCCATATTCC	Generation of transgenic plants	
R: <u>CGGGATCC</u> TATATATGGAGATTTAATTTGC		
<i>DkACTIN</i>	F: TGCTCTTCCAGCCATCACTCATT	RT-qPCR
	R: ATTTCCTTGCTCATCCGGTCAG	
<i>AtACTIN2</i>	F: TTGTGCTGGATTCTGGTGATGGT	RT-qPCR
	R: CCGCTCTGCTGTTGTGGTGAA	
<i>AtSAG12</i>	F: GGATGTCCCGTTAATGATG	RT-qPCR
	R: TCCACTTTCTCCCATTTTG	
<i>AtSAG13</i>	F: GCTGTGGTGGAGGAAGTAGC	RT-qPCR
	R: CCACATTGTTGACGAGGATG	
<i>LeUBI3</i>	F: CTACAACATCCAGAAGG	RT-qPCR
	R: TGCAACACAGCGAGCTTAACC	
<i>LeACS2</i>	F: CCTCACCATTAGTTCGTTAAGACT	RT-qPCR
	R: CCTCACCATTAGTTCGTTAAGACT	
<i>LeACS4</i>	F: GCAAGGATTCGGATGTTATGGATGC	RT-qPCR
	R: TGCTCGCACTACGAGCGAGGAATTG	
<i>LeACO1</i>	F: ACACGAATGTCAGCTCAT	RT-qPCR
	R: TCCATTGCCTCATTGCTTCAA	

**Table 1. Oligonucleotide sequences for primers used in this study.** <sup>a</sup>Letters “F” and “R” indicate the forward and reverse primers, respectively.

sequences were digested with *Xba*I and *Kpn*I and then inserted into the pBI 221-GFP vector. After bombardment and cultivation, the onion epidermal cells were imaged using a confocal laser-scanning microscope. A Nikon A1 confocal microscope system operating on a Ti-E inverted microscope and equipped with a Plan Apo 10x microscope objective (Nikon, Tokyo, Japan) was used for this study. The confocal settings were excitation at 488 nm and emission wavelength was 525 nm. Images were obtained with 1x zoom and recorded at high resolution (2 comps 12 bit) using 2-fold line averaging. When indicated, cells were plasmolyzed in 400 mM sucrose for 15 min.

**Production and purification of recombinant XTH proteins and enzyme activity analysis.** The coding region of *DkXTH8* without the signal peptide sequence was amplified using combinations of specific primers (Table 1). After confirmation, the products were digested with *Bam*HI and *Hind*III and ligated into the pET-32a vector. The recombinant plasmid DkXTH8- pET-32a was introduced into *Escherichia coli* BL21 via the heat-shock method, and expression of the recombinant protein was induced with 0.100 mM isopropyl  $\beta$ -D-thiogalactopyranoside at 16 °C for 68 h with shaking at 20 revs<sup>-1</sup>. After sonication, the bacterial cell lysate was centrifuged for 10 minutes at 10,000  $\times$  g. Subsequently, the crude proteins in the supernatant were concentrated and dissolved in binding-wash buffer (40 mM Tris-HCl, 0.5 M NaCl, 20 mM imidazole, 10% glycerol, pH 7.9) and purified on a nickel-nitrilotriacetic acid (Ni-NTA) resin column. The pET-32a vector alone was used as the blank control. After analysis by SDS-polyacrylamide gel electrophoresis, DkXTH8-RP was concentrated and dialyzed in citrate/phosphate buffer (pH 5.5) for determination of XET/XEH activity according to Han *et al.*<sup>27</sup>.

**Generation of transgenic *Arabidopsis* and tomato plants overexpressing *DkXTH8*.** The coding region of *DkXTH8* was amplified by PCR using the primers listed in Table 1. After digestion with the corresponding restriction enzymes (underlined in the primers), the resulting PCR products were inserted into the *Bam*HI- and *Xba*I-digested binary vector 35 S:pVBG2307 (Fig. S1a). The recombinant plasmid DkXTH8-pVBG2307



was then introduced into *Agrobacterium tumefaciens* GV3101. *A. thaliana* ecotype ‘Columbia’ was transformed via the floral dip method<sup>49</sup>, and T3 homozygous transgenic lines (AL1, AL2 and AL3) were generated. Cultivar Micro-Tom was transformed via *Agrobacterium*-mediated leaf transformation as described by Hou *et al.*<sup>28</sup>, and T1 transgenic lines (TL1, TL2 and TL3) were used.

**Dark-induced *Arabidopsis* leaf senescence.** The fifth–sixth leaves of 4-week-old *Arabidopsis* plants were detached according to Hou *et al.*<sup>28</sup>. The leaves were floated on water in 9-mm-diameter Petri dishes and stored for up to 4 d in the dark at 22 °C to promote senescence. Detached leaves stored under growth conditions (16 h of light at 22 °C and 8 h of dark at 18 °C) served as the control.

**Measurements of the chlorophyll content and relative electrolyte leakage.** The chlorophyll concentration was determined spectrophotometrically as described by Wellburn<sup>50</sup>.

For the relative electrolyte leakage measurement, collected leaves were cut into discs (5 mm in diameter). After vacuum-infiltration of deionized water for 30 min, 10 discs were incubated in 5 mL ddH<sub>2</sub>O for 2 h. The initial conductivities (C1) of the solutions were measured using a conductivity meter. The samples were then boiled for 15 min and cooled to room temperature for recording the final conductivities (C2). The relative electrolyte leakage is expressed as C1/C2.

**Storage of transgenic tomato fruits.** Tomato fruits of WT and *DkXTH8*-transgenic lines were collected at the mature green period with no obvious color change. For postharvest softening and senescence analyses, fruits from each group were divided randomly into three subgroups, and all groups were stored at 25 ± 1 °C and 85–95% relative humidity. To investigate fruit color, a chroma meter CR-400 (Konica Minolta, Osaka, Japan) equipped with an 8-mm-diameter measuring area in the head was used.

**Microscopic observation of WT and *DkXTH8*-transgenic plants.** The fifth–sixth mature leaves (0.5 × 0.5 cm) and stems (0.5 cm) at 1–2 cm height above the ground were obtained from *Arabidopsis* WT and *DkXTH8*-transgenic line AL2 at four weeks after sowing. Tomato fruit materials (approximately 2 mm<sup>3</sup>) were collected from WT and *DkXTH8*-transgenic line TL1, as described in 4.11. The samples were immediately fixed in FAA solution (2% formaldehyde, 5% acetic acid, and 63% ethanol), placed under vacuum for 1 h and then processed as follows: dehydration in 70%, 85%, 95% and 100% ethanol (1 h each step); vitrified with a gradient from 100% ethanol to 100% xylene; infiltrated and embedded in paraffin. The polymerized samples were cut into 8-μm thick sections using a microtome (Leica RM2016, Germany) and then mounted onto microscopic slides. After staining with safranin, the samples were examined by light microscopy and imaged by confocal laser-scanning microscopy (T2; Olympus, Tokyo, Japan).

**Statistical analysis.** Data were evaluated by analysis of variance (ANOVA) using SPSS Statistics 22.0 software, and the means were compared by Fisher’s least significant difference (LSD) test. *P* values below 0.05 were considered statistically significant (*P* < 0.05). The data are expressed as the mean ± standard error.

## References

- Cosgrove, D. J. Growth of the plant cell wall. *Nature Reviews Molecular Cell Biology* **6**, 850–861, doi: 10.1038/nrm1746 (2005).
- Figuroa, C. R. *et al.* Softening rate of the Chilean strawberry (*Fragaria chiloensis*) fruit reflects the expression of polygalacturonase and pectate lyase genes. *Postharvest Biology and Technology* **49**, 210–220, doi: 10.1016/j.postharvbio.2008.01.018 (2008).
- Payasi, A., Mishra, N. N., Chaves, A. L. S. & Singh, R. Biochemistry of fruit softening: an overview. *Physiol. Mol. Biol. Plants* **15**, 103–113, doi: 10.1007/s12298-009-0012-z (2009).
- Brummell, D. A. & Harpster, M. H. Cell wall metabolism in fruit softening and quality and its manipulation in transgenic plants. *Plant Molecular Biology* **47**, 311–340, doi: 10.1023/a:1010656104304 (2001).
- Schroder, R., Atkinson, R. G., Langenkamper, G. & Redgwell, R. J. Biochemical and molecular characterisation of xyloglucan endotransglycosylase from ripe kiwifruit. *Planta* **204**, 242–251, doi: 10.1007/s004250050253 (1998).
- Zhu, Q. *et al.* Identification of xyloglucan endotransglucosylase/hydrolase genes (XTHs) and their expression in persimmon fruit as influenced by 1-methylcyclopropene and gibberellic acid during storage at ambient temperature. *Food Chemistry* **138**, 471–477, doi: 10.1016/j.foodchem.2012.09.141 (2013).
- Nishitani, K. In *International Review of Cytology - a Survey of Cell Biology*, Vol 173 Vol. 173 *International Review of Cytology - a Survey of Cell Biology* (ed. K. W. Jeon) 157–206 (1997).
- Saladie, M., Rose, J. K., Cosgrove, D. J. & Catala, C. Characterization of a new xyloglucan endotransglucosylase/hydrolase (XTH) from ripening tomato fruit and implications for the diverse modes of enzymic action. *The Plant Journal: for cell and molecular biology* **47**, 282–295, doi: 10.1111/j.1365-313X.2006.02784.x (2006).
- Rose, J. K. C., Braam, J., Fry, S. C. & Nishitani, K. The XTH family of enzymes involved in xyloglucan endotransglucosylation and endohydrolysis: Current perspectives and a new unifying nomenclature. *Plant and Cell Physiology* **43**, 1421–1435, doi: 10.1093/pcp/pcf171 (2002).
- Eklof, J. M. & Brumer, H. The XTH Gene Family: An Update on Enzyme Structure, Function, and Phylogeny in Xyloglucan Remodeling. *Plant Physiology* **153**, 456–466, doi: 10.1104/pp.110.156844 (2010).
- Campbell, P. & Braam, J. Xyloglucan endotransglucosylases: diversity of genes, enzymes and potential wall-modifying functions. *Trends in Plant Science* **4**, 361–366, doi: 10.1016/s1360-1385(99)01468-5 (1999).
- Yokoyama, R. & Nishitani, K. Functional diversity of xyloglucan-related proteins and its implications in the cell wall dynamics in plants. *Plant Biology* **2**, 598–604, doi: 10.1055/s-2000-16643 (2000).
- Fry, S. C. Primary cell wall metabolism: tracking the careers of wall polymers in living plant cells. *New Phytologist* **161**, 641–675, doi: 10.1111/j.1469-8137.2003.00980.x (2004).
- Xu, W., Campbell, P., Vargheese, A. K. & Braam, J. The *Arabidopsis* XET-related gene family: Environmental and hormonal regulation of expression. *Plant Journal* **9**, 879–889, doi: 10.1046/j.1365-313X.1996.9060879.x (1996).
- Xu, W. *et al.* *Arabidopsis* TCH4, regulated by hormones and the environment, encodes a xyloglucan endotransglucosylase. *Plant Cell* **7**, 1555–1567 (1995).

16. Singh, A. P., Tripathi, S. K., Nath, P. & Sane, A. P. Petal abscission in rose is associated with the differential expression of two ethylene-responsive xyloglucan endotransglucosylase/hydrolase genes, RbXTH1 and RbXTH2. *J. Exp. Bot.* **62**, 5091–5103, doi: 10.1093/jxb/err209 (2011).
17. Liu, Y.-B., Lu, S.-M., Zhang, J.-F., Liu, S. & Lu, Y.-T. A xyloglucan endotransglucosylase/hydrolase involves in growth of primary root and alters the deposition of cellulose in Arabidopsis. *Planta* **226**, 1547–1560, doi: 10.1007/s00425-007-0591-2 (2007).
18. Potter, I. & Fry, S. C. Xyloglucan endotransglucosylase activity in pea internodes - effects of applied gibberellic-acid. *Plant Physiology* **103**, 235–241, doi: 10.1104/pp.103.1.235 (1993).
19. Feng, H.-L. *et al.* Differential expression and regulation of longan XET genes in relation to fruit growth. *Plant Science* **174**, 32–37, doi: 10.1016/j.plantsci.2007.09.008 (2008).
20. Ishimaru, M. & Kobayashi, S. Expression of a xyloglucan endo-transglycosylase gene is closely related to grape berry softening. *Plant Science* **162**, 621–628, doi: 10.1016/s0168-9452(01)00608-2 (2002).
21. Ishimaru, M., Smith, D. L., Gross, K. C. & Kobayashi, S. Expression of three expansin genes during development and maturation of Kyoho grape berries. *J. Plant Physiol.* **164**, 1675–1682, doi: 10.1016/j.jplph.2006.07.017 (2007).
22. Munoz-Bertomeu, J., Miedes, E. & Lorences, E. P. Expression of xyloglucan endotransglucosylase/hydrolase (XTH) genes and XET activity in ethylene treated apple and tomato fruits. *Journal of plant physiology* **170**, 1194–1201, doi: 10.1016/j.jplph.2013.03.015 (2013).
23. Percy, A. E. *et al.* Xyloglucan endotransglucosylase activity during fruit development and ripening of apple and kiwifruit. *Physiol. Plant.* **96**, 43–50 (1996).
24. Miedes, E. *et al.* Xyloglucan endotransglucosylase and cell wall extensibility. *J. Plant Physiol.* **168**, 196–203, doi: 10.1016/j.jplph.2010.06.029 (2011).
25. Ohba, T., Takahashi, S. & Asada, K. Alteration of fruit characteristics in transgenic tomatoes with modified expression of a xyloglucan endotransglucosylase/hydrolase gene. *Plant Biotechnology* **28**, 25–32, doi: 10.5511/plantbiotechnology.10.0922a (2011).
26. Miedes, E., Herbers, K., Sonnewald, U. & Lorences, E. P. Overexpression of a cell wall enzyme reduces xyloglucan depolymerization and softening of transgenic tomato fruits. *Journal of agricultural and food chemistry* **58**, 5708–5713, doi: 10.1021/jf100242z (2010).
27. Han, Y. *et al.* Analysis of Xyloglucan Endotransglucosylase/Hydrolase (XTH) Genes and Diverse Roles of Isoenzymes during Persimmon Fruit Development and Postharvest Softening. *Plos One* **10**, doi: 10.1371/journal.pone.0123668 (2015).
28. Hou, Y. *et al.* The Persimmon 9-lipoxygenase Gene DkLOX3 Plays Positive Roles in Both Promoting Senescence and Enhancing Tolerance to Abiotic Stress. *Frontiers in Plant Science* **6**, doi: 10.3389/fpls.2015.01073 (2015).
29. Lv, J. *et al.* Cloning and expression of lipoxygenase genes and enzyme activity in ripening persimmon fruit in response to GA and ABA treatments. *Postharvest Biology and Technology* **92**, 54–61, doi: 10.1016/j.postharvbio.2014.01.015 (2014).
30. Johansson, P. *et al.* Crystal structures of a poplar xyloglucan endotransglucosylase reveal details of transglycosylation acceptor binding. *Plant Cell* **16**, 874–886, doi: 10.1105/tpc.020065 (2004).
31. Baumann, M. J. *et al.* Structural evidence for the evolution of xyloglucanase activity from xyloglucan endo-transglycosylases: Biological implications for cell wall metabolism. *Plant Cell* **19**, 1947–1963, doi: 10.1105/tpc.107.051391 (2007).
32. Kallas, A. M. *et al.* Enzymatic properties of native and deglycosylated hybrid aspen (*Populus tremula* x *tremuloides*) xyloglucan endotransglucosylase 16A expressed in *Pichia pastoris*. *Biochemical Journal* **390**, 105–113, doi: 10.1042/bj20041749 (2005).
33. Concha, C. M. *et al.* Methyl jasmonate treatment induces changes in fruit ripening by modifying the expression of several ripening genes in *Fragaria chiloensis* fruit. *Plant Physiology and Biochemistry* **70**, 433–444, doi: 10.1016/j.plaphy.2013.06.008 (2013).
34. Han, Y. *et al.* Isolation and Characterization of Two Persimmon Xyloglucan Endotransglucosylase/Hydrolase (XTH) Genes That Have Divergent Functions in Cell Wall Modification and Fruit Postharvest Softening. *Frontiers in Plant Science* **7**, doi: 10.3389/fpls.2016.00624 (2016).
35. Zhu, X. *et al.* Molecular cloning, characterizing, and expression analysis of CTR1 genes in harvested papaya fruit. *European Food Research and Technology* **238**, 503–513, doi: 10.1007/s00217-013-2131-6 (2014).
36. Li, C.-r. *et al.* 1-MCP delayed softening and affected expression of XET and EXP genes in harvested cherimoya fruit. *Postharvest Biology and Technology* **52**, 254–259, doi: 10.1016/j.postharvbio.2008.12.009 (2009).
37. Tabuchi, A., Mori, H., Kamisaka, S. & Hoson, T. A new type of endo-xyloglucan transferase devoted to xyloglucan hydrolysis in the cell wall of azuki bean epicotyls. *Plant and Cell Physiology* **42**, 154–161, doi: 10.1093/pcp/pce016 (2001).
38. Steele, N. M. & Fry, S. C. Differences in catalytic properties between native isoenzymes of xyloglucan endotransglucosylase (XET). *Phytochemistry* **54**, 667–680, doi: 10.1016/s0031-9422(00)00203-x (2000).
39. Sulova, Z., Baran, R. & Farkas, V. Divergent modes of action on xyloglucan of two isoenzymes of xyloglucan endo-transglycosylase from *Tropaeolum majus*. *Plant Physiology and Biochemistry* **41**, 431–437, doi: 10.1016/s0981-9428(03)00050-0 (2003).
40. Atkinson, R. G., Johnston, S. L., Yauk, Y.-K., Sharma, N. N. & Schroder, R. Analysis of xyloglucan endotransglucosylase/hydrolase (XTH) gene families in kiwifruit and apple. *Postharvest Biology and Technology* **51**, 149–157, doi: 10.1016/j.postharvbio.2008.06.014 (2009).
41. Maris, A., Suslov, D., Fry, S. C., Verbelen, J.-P. & Vissenberg, K. Enzymic characterization of two recombinant xyloglucan endotransglucosylase/hydrolase (XTH) proteins of Arabidopsis and their effect on root growth and cell wall extension. *J. Exp. Bot.* **60**, 3959–3972, doi: 10.1093/jxb/erp229 (2009).
42. Bollok, M. *et al.* Production of poplar xyloglucan endotransglucosylase using the methylotrophic yeast *Pichia pastoris*. *Applied Biochemistry and Biotechnology* **126**, 61–77, doi: 10.1007/s12010-005-0006-4 (2005).
43. Genovesi, V. *et al.* ZmXTH1, a new xyloglucan endotransglucosylase/hydrolase in maize, affects cell wall structure and composition in Arabidopsis thaliana. *Journal of experimental botany* **59**, 875–889, doi: 10.1093/jxb/ern013 (2008).
44. Han, Y. *et al.* *Populus euphratica* XTH overexpression enhances salinity tolerance by the development of leaf succulence in transgenic tobacco plants. *J. Exp. Bot.* **64**, 4225–4238, doi: 10.1093/jxb/ert229 (2013).
45. Quirino, B. F., Noh, Y. S., Himelblau, E. & Amasino, R. M. Molecular aspects of leaf senescence. *Trends in Plant Science* **5**, 278–282, doi: 10.1016/s1360-1385(00)01655-1 (2000).
46. Strother, S. The role of free radicals in leaf senescence. *Gerontology* **34**, 151–156 (1988).
47. Wagstaff, C. *et al.* Modification of cell wall properties in lettuce improves shelf life. *J. Exp. Bot.* **61**, 1239–1248, doi: 10.1093/jxb/erq038 (2010).
48. Livak, K. J. & Schmittgen, T. D. Analysis of relative gene expression data using real-time quantitative PCR and the 2<sup>-</sup>(Delta Delta C(T)) Method. *Methods* **25**, 402–408, doi: 10.1006/meth.2001.1262 (2001).
49. Clough, S. J. & Bent, A. F. Floral dip: a simplified method for Agrobacterium-mediated transformation of Arabidopsis thaliana. *Plant Journal* **16**, 735–743, doi: 10.1046/j.1365-313x.1998.00343.x (1998).
50. Wellburn, A. R. The spectral determination of chlorophyll-a and chlorophyll-b, as well as total carotenoids, using various solvents with spectrophotometers of different resolution. *J. Plant Physiol.* **144**, 307–313 (1994).

## Acknowledgements

This work was supported by National Key Research and Development Program (2016YFD0400102). We thank Prof. Zhenhui Gong (Northwest A&F University, China) for providing the pVBG2307 vector.

### Author Contributions

Y.Han and J.R. conceived and designed research. Y.Han and Q.B. conducted experiments. Y.Han, Q.B. and H.L. analyzed data. Y.Hou, M.J. and S.H. contributed new reagents or analytical tools. Y.Han and Q.B. wrote the manuscript. The work has not been submitted elsewhere for publication, and all the authors listed have approved the manuscript that is enclosed.

### Additional Information

**Supplementary information** accompanies this paper at <http://www.nature.com/srep>

**Competing financial interests:** The authors declare no competing financial interests.

**How to cite this article:** Han, Y. *et al.* DkXTH8, a novel xyloglucan endotransglucosylase/hydrolase in persimmon, alters cell wall structure and promotes leaf senescence and fruit postharvest softening. *Sci. Rep.* **6**, 39155; doi: 10.1038/srep39155 (2016).

**Publisher's note:** Springer Nature remains neutral with regard to jurisdictional claims in published maps and institutional affiliations.



This work is licensed under a Creative Commons Attribution 4.0 International License. The images or other third party material in this article are included in the article's Creative Commons license, unless indicated otherwise in the credit line; if the material is not included under the Creative Commons license, users will need to obtain permission from the license holder to reproduce the material. To view a copy of this license, visit <http://creativecommons.org/licenses/by/4.0/>

© The Author(s) 2016